IRSTI 31.15.37 https://doi.org/10.26577/phst20261315

Synthesis of a montmorillonite-based nanocomposite with antibacterial properties

D.K. Bolatkan[1*], K. Akatan[1], S.K. Kabdrakhmanova[2*], V.V. Davydova[3] and Sh.A. Muzdybayeva[4]

[1]S.Amanzholov East Kazakhstan University, Ust-Kamenogorsk, Kazakhstan
[2]Satbayev University, Almaty, Kazakhstan
[3]International R&D Center for Advanced Functional Materials and their Composite, Almaty, Kazakhstan
[4]International Engineering Technological University, Almaty, Kazakhstan
*e-mail: chilibayeva35@gmail.com

(Received March 31, 2026; received in revised form May 18, 2026; accepted May 28, 2026)

This study investigates the intercalation of montmorillonite clays from the Tagan deposit with silver nanoparticles and evaluates their potential for biomedical applications. Purification of the raw material using the Salo method ensured the removal of coarse mineral impurities and enrichment of the montmorillonite fraction. The analyses revealed the predominance of montmorillonite and kaolinite in the purified samples, while SEM data confirmed increased porosity and effective distribution of silver nanoparticles within the interlayer space. Modification resulted in the formation of a hybrid structure with high surface reactivity, allowing the material to be considered a promising carrier for the immobilization and controlled release of pharmaceutical substances. In addition, the modified bentonite may be used in antimicrobial coatings, wound-healing materials, drug delivery systems, medicinal ointments, as well as in sorption and environmental protection technologies. The incorporation of silver nanoparticles also enhanced the antibacterial potential of the clay matrix, which is particularly important for the development of advanced biomedical and healthcare-related materials. Furthermore, the combination of natural clay minerals with nanoscale silver provides a cost-effective and environmentally friendly platform for creating multifunctional composites with improved physicochemical and biological properties. The results confirm that purification and functionalization with silver nanoparticles significantly improve the properties of these clays and expand their potential practical applications.

Keywords: montmorillonite, silver nanoparticles, green method, antibacterial properties, nanocomposite.

1. Introduction

The widespread application of montmorillonite clays is determined by their distinctive physicochemical properties, natural abundance, and environmental safety [1]. In recent years, the growing interest in the use of polymer–clay nanocomposites in drug delivery systems has made montmorillonite-based materials a relevant subject of biomedical research [2]. Montmorillonite is the principal mineralogical component of bentonite and, as a layered aluminosilicate belonging to the smectite group, is distinguished by its high sorption capacity, pronounced adsorption activity, and considerable swelling ability [3]. However, the presence of kaolinite, quartz, mica, calcite, and other mineral impurities in natural bentonites may reduce their degree of purity and functional performance. In addition, coarse dispersed impurities such as sand and stone disrupt the structural homogeneity of the clay matrix, thereby limiting the material's biomedical applicability[4]. Therefore, their preliminary removal is of critical importance [4]. For this reason, thorough purification and targeted pretreatment of the raw material play a decisive role in the production of bentonite-based materials intended for medical applications [5-6]. Purified bentonite exhibits high adsorption capacity, biocompatibility, and the ability to control the release of immobilized active components [7]. In this regard, it is regarded as an effective carrier material for the development of solid dosage forms, including tablets and capsules [8]. Studies [9-10] have reported that montmorillonites have increasingly been used as potential raw materials for the formulation of deep-cleansing facial

masks and skincare creams due to their safety, bioinertness, and environmental friendliness.

Recent studies have demonstrated that the effective functionalization of the interlayer space of bentonite with nanoparticles enables the targeted modification of its properties and the expansion of its application potential [11]. Although purified bentonite possesses a large specific surface area, high cation-exchange capacity, and good biocompatibility, its antibacterial activity remains limited. Studies [12–13] have shown that modification with silver and copper nanoparticles significantly enhances the functional characteristics of bentonite, including its antimicrobial activity. In this context, the interlayer space of bentonite serves as a favorable structural environment for the incorporation of metal nanoparticles. The incorporated metal atoms combine to form nanoparticles and establish stable interactions with the layers of the clay mineral. As a result of such interactions, silver nanoparticles become immobilized within the interlayer region, thereby preventing the formation of low-activity aggregates and conglomerates. This process is accomplished through a spontaneous cation-exchange mechanism. It has been concluded that this contributes to enhancing the stability and biological activity of nanocomposites based on modified bentonite.

In recent years, montmorillonite clay has been considered a promising inorganic matrix for the development of antibacterial nanocomposites due to its layered structure, high cation-exchange capacity, availability, and ability to stabilize metallic nanoparticles. Of particular interest are AgNP–MMT systems, in which silver nanoparticles can be intercalated into the interlayer space of montmorillonite. This may reduce AgNP aggregation, improve their dispersion, and contribute to prolonged antibacterial activity. According to recent literature data, silver-containing montmorillonite materials exhibit antibacterial activity against both Gram-positive and Gram-negative microorganisms, making them promising for biomedical, packaging, and environmental applications. In addition, the use of "green" synthesis methods involving plant extracts or mild reducing approaches can reduce the use of toxic reagents and improve the environmental safety of AgNP–MMT nanocomposite preparation. Recently, in accordance with the principles of green chemistry, priority has been given to the green synthesis of metal nanoparticles incorporated into antibacterial composites intended for biomedical applications [14]. Recent studies have demonstrated that nanostructured materials prepared by environmentally friendly approaches can exhibit promising properties for biomedical and bioimaging applications, highlighting the importance of particle size, surface chemistry, and biocompatibility for their practical use [15-17].This, in turn, has been found to ensure the environmentally safe use of synthesized metal nanoparticles and to maximize the safety of their application. The novelty of this study lies in the use of local bentonite clay from the Tagan deposit, with montmorillonite as the main mineral component, as a carrier matrix for silver nanoparticles. Unlike previously reported AgNP–montmorillonite systems, the present work focuses on the intercalation of green-synthesized silver nanoparticles into a local natural bentonite clay and the evaluation of the antibacterial properties of the obtained material. Thus, the study combines the use of regional mineral raw material, an environmentally friendly synthesis approach, and the development of a silver-containing bentonite material with potential antibacterial activity.

Accordingly, the present study aimed to investigate the possibility of obtaining an antibacterial nanocomposite by preliminary water activation of natural bentonite samples from the Tagan deposit and subsequent intercalation of green-synthesized silver nanoparticles into the bentonite matrix.

2. Experimental section

2.1 Pretreatment of bentonite clay

Bentonite samples obtained from the Tagan deposit were selected as the study material and prepared as a suspension in deionized water at a ratio of 1:20 g/mL, following the procedure reported in our previous study [4]. The obtained suspension was magnetically stirred at room temperature at 1000 rpm for 8 h, followed by treatment at 90 °C for 2 h. The resulting suspension was then lyophilized at −60 °C for 5 h.

2.2 Intercalation of silver nanoparticles synthesized via a green method into the montmorillonite matrix

Silver nanoparticles synthesized via the green method reported in study [18] were intercalated into the montmorillonite matrix. The required concentration was prepared using two different approaches. In the first method, 5 g of water-modified bentonite clay was added to silver nanoparticle suspensions with volumes of 25, 50, and 75 mL (samples 1-6), followed by continuous stirring on a magnetic stirrer. In the second method, silver nanoparticles were added to the aqueous swollen clay suspension at volume ratios of 1:3, 1:1, and 3:1 (mL/mL) and intercalated under continuous stirring (samples 7-12).

The bentonite samples investigated in this work were conventionally labeled as Mt_1 and Mt_2, while the nanocomposite clay samples intercalated with silver nanoparticles were designated as Mt_1-AgNPs and Mt_2-AgNPs. Depending on the nature of the analysis, either the suspension of modified montmorillonite clay or its lyophilized dry form was employed.

2.3 Determination of the microbiological purity of montmorillonite clay and the antibacterial properties of the obtained nanocomposite clay

The antibacterial properties and microbiological purity were determined by the inoculation method in accordance with the requirements of the State Pharmacopoeia of the Republic of Kazakhstan (pp. 176–180, Section 2.6.12). A suspension was prepared by adding 1 g of the nanocomposite to 9 mL of 0.9% sodium chloride solution containing peptone at pH 7, followed by intensive mixing. During the study, the suspension was subjected to a tenfold dilution.

A 1 mL aliquot of the tenfold diluted suspension was transferred into 90 mm Petri dishes, after which 15–20 mL of molten culture medium at a temperature not exceeding 45 °C was poured onto the sample. Meat-peptone agar was used for bacterial cultivation, whereas Sabouraud medium was employed for the cultivation of molds and yeasts. The bacterial strains were incubated at 30–35 °C for 48 h, while the molds were incubated at 20–25 °C for 5 days.

Colony counting was performed on plates containing 30–300 colonies for bacteria and 10–100 colonies for fungi. The number of viable microorganisms (CFU/mL) was calculated taking into account the dilution factor and the volume of the inoculated sample. The average value of two parallel analyses was used for the calculations.

The concentration of viable microorganisms was calculated using the following formula:

$$N = \frac{C}{V} * \frac{1}{d} \quad (1)$$

where N is the concentration of microorganisms in the initial sample (CFU/mL), C is the number of colonies on the plate, V is the volume of the inoculated sample (mL), and d is the dilution factor.

2.4 FTIR spectroscopy

The chemical structure of the samples was investigated using an FTIR FT-801 infrared spectrometer (Simex, Russia) in the 500–4000 cm^{-1} wavenumber range, with a resolution of 1 cm^{-1}, at 25 ± 2 °C, using 100 scans. During the analysis, the clay powders were mixed with potassium bromide at a 1:9 ratio and ground in an agate mortar until a completely homogeneous mixture was obtained. The resulting mixture was then placed in a pellet-forming ring and compressed using a press at 200 MPa for 5 min, while water vapor was removed by a vacuum pump, to obtain a pellet.

2.5 X-ray fluorescence analysis

The major elemental composition of bentonite clay was determined by energy-dispersive X-ray fluorescence (EDXRF) using an Epsilon 4 X-ray fluorescence spectrometer (Malvern Panalytical B.V., Almelo, The Netherlands). Measurements were carried out using an Ag-anode X-ray tube and an SDD detector, at an accelerating voltage range of 4.0–50 kV and a current of up to 3.0 mA. The samples were analyzed in powdered form as pressed pellets. The results were presented as elemental concentrations.

2.6 X-ray diffraction analysis

The structural and phase characteristics of the samples were investigated by X-ray diffraction using an X'PertPRO diffractometer (Malvern Panalytical Empyrean, The Netherlands) with monochromatized CuKα radiation (K-Alpha1 [Å] = 0.1542) at a scanning step size of 0.02°. During the analysis, the measurements were carried out over an angular range of 10–80°, with an X-ray tube voltage of 45 kV, a current of 30 mA, and a counting time of 0.5 s per step; a universal aluminum sample holder (PW1172/01) was used.

2.7 SEM analysis

The surface morphology of the samples was examined using a Quanta 200 3D scanning electron microscope (FEI™, Netherlands). The measurements were performed in high-vacuum mode at an accelerating voltage of 5 kV, using a secondary electron detector. To improve electron conductivity, the surface of the mineral clays was coated with gold nanoparticles.

2.8 Viscosity of the nanocomposite

The dynamic viscosity of the samples was determined using a rotational viscometer (BOYN, Hangzhou Boyn Instrument Co., Ltd., China). The analysis was performed at a temperature of 25 ± 2 °C and a relative humidity of 50 ± 5%. The sample was placed in the measuring vessel, and care was taken to prevent the formation of air bubbles. The spindle was immersed into the sample up to the working level, and the measurement was carried out at a rotational speed selected in accordance with the technical oper-

ating mode of the instrument. After the readings had stabilized, the viscosity value was recorded in mPa·s. To ensure measurement repeatability and comparability of the results, all analyses were performed under identical experimental conditions. Each sample was measured at least three times, and the results were processed as the mean ± standard deviation.

3. Results and discussion

3.1 Assessment of the microbiological purity of montmorillonite clay and the antibacterial activity of the obtained nanocomposite clay

According to the requirements of the State Pharmacopoeia of the Republic of Kazakhstan, the analysis of the microbiological purity of the purified clay samples Mt_1 and Mt_2 revealed a total aerobic microbial count of 0.92×10^4 CFU/g. This value did not exceed the permissible limit ($\leq 1 \times 10^4$ CFU/g). The yeast and mold count was 0.95×10^2 CFU/g, which also remained within the acceptable range ($\leq 1 \times 10^2$ CFU/g).

For the Mt_2 clay sample, the total aerobic microbial count was 0.89×10^4 CFU/g, while the yeast and mold count was 0.8×10^2 CFU/g. These values fully complied with the pharmacopoeial requirements. The obtained results demonstrated that the studied samples complied with the requirements of the State Pharmacopoeia of the Republic of Kazakhstan for non-sterile medicinal products of natural origin. In addition, these results were consistent with the data reported in study [4] regarding the microbiological purity of montmorillonite clay. Thus, it was confirmed that the samples used in the present study possessed the microbiological purity characteristic of montmorillonite clays.

Figure 1 presents the antibacterial properties of the initial montmorillonite clay samples, Mt_1 and Mt_2, as well as those of the nanocomposite samples obtained after intercalation. No inhibition zones were observed for either Mt_1 or Mt_2 clay against the tested microorganisms. For series 1–3 and 4–6 of the nanocomposite clay samples, a clear trend was observed toward an increase in the microbial growth inhibition zone with increasing volume of AgNPs in the solution. In sample No. 3 (Mt1 + 75 mL AgNPs), the inhibition zone reached 11 mm, whereas in sample No. 6 (Mt2 + 75 mL AgNPs), it was 11.2 mm. A similar relationship was also observed for the mixed compositions of samples 7–9 and 10–12. This indicates the dose-dependent nature of the antibacterial effect of AgNPs. Comparative analysis showed that the antibacterial activity of the studied compositions against Escherichia coli and Staphylococcus saprophyticus was generally comparable.

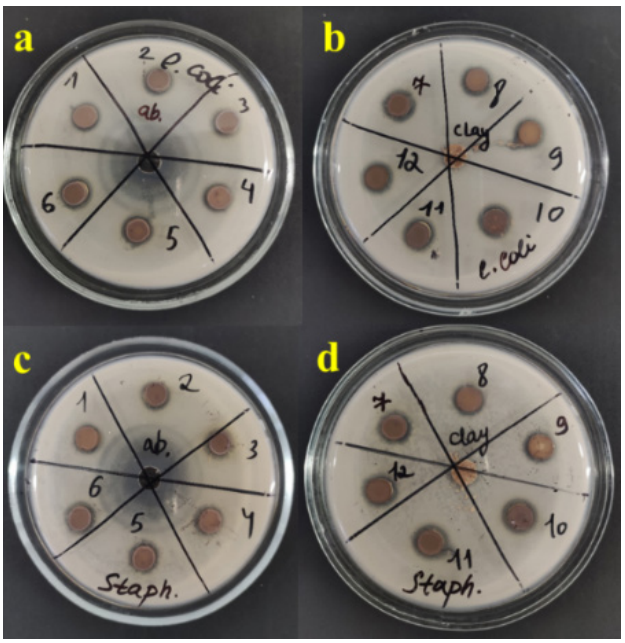

Figure 1. Results of the antibacterial activity assay. Inhibition zones against E. coli: (a) samples 1–6 and (b) samples 7–12; inhibition zones against S. saprophyticus: (c) samples 1–6 and (d) samples 7–12.

Table 1. Antibacterial activity of the nanocomposite clay.

Sample numbers	Sample designation	Average ± SEM (mm)	
		Escherichia coli	*Staphylococcus saprophyticus*
5 g of dry, purified montmorillonite clay and various concentrations of AgNPs			
1	Mt_1 + 25 ml AgNPs	10.00 ± 0.06^b	10.00 ± 0.07^b
2	Mt_1+ 50 ml AgNPs	10.40 ± 0.07^b	10.50 ± 0.06^b
3	Mt_1 + 75 ml AgNPs	11.00 ± 0.08^a	10.70 ± 0.07^{ab}
4	Mt_2 + 25 ml AgNPs	10.00 ± 0.06^b	10.30 ± 0.08^b

Continuation of the table

Sample numbers	Sample designation	Average ± SEM (mm)	
		Escherichia coli	*Staphylococcus saprophyticus*
5	Mt_2 + 50 ml AgNPs	10.30 ± 0.07[b]	10.20 ± 0.06[b]
6	Mt_2 + 75 ml AgNPs	11.20 ± 0.09[a]	11.40 ± 0.08[a]
Addition of AgNPs to the bentonite clay suspension in different volumes			
7	30 ml Mt_2 + 70 ml AgNPs	11.00 ± 0.07[a]	10.50 ± 0.06[b]
8	50 ml Mt_2 + 50 ml AgNPs	10.00 ± 0.06[b]	10.00 ± 0.07[b]
9	70 ml Mt_2 + 30 ml AgNPs	10.00 ± 0.07[b]	9.50 ± 0.08[c]
10	30 ml Mt_1 + 70 ml AgNPs	11.00 ± 0.08[a]	11.00 ± 0.07[a]
11	50 ml Mt_1 + 50 ml AgNPs	10.00 ± 0.06[b]	10.70 ± 0.08[ab]
12	70 ml Mt_1 + 30 ml AgNPs	9.70 ± 0.07[c]	10.50 ± 0.06[b]

The control samples consisting of the pristine clay did not exhibit any inhibitory activity. In contrast, the nanocomposite material intercalated with silver nanoparticles demonstrated pronounced antibacterial activity. These results indicate that silver nanoparticles play a decisive role in the development of antibacterial activity [18]. The results of the study revealed that the sample containing 5 g of montmorillonite clay intercalated with 75 mL of silver nanoparticles exhibited the highest antimicrobial activity. In addition, considering that the Mt_1 and Mt_2 samples met the requirements for microbiological purity, these two montmorillonite clay samples and this specific ratio with silver nanoparticles were selected as the basis for the subsequent synthesis of the nanocomposite material.

A clay–water system was used as a negative control to confirm that the pristine clay matrix itself did not exhibit antibacterial activity. No inhibition zone was observed for this control sample, indicating that the unmodified clay did not significantly suppress microbial growth. Erythromycin was used as a positive control to confirm the viability of the tested microorganisms and the correctness of the agar diffusion method. The inhibition zone of erythromycin was 22.1 mm, while the Mt_2-AgNPs sample obtained using 75 mL of AgNPs solution showed an inhibition zone of 11.2 mm.

For a more quantitative comparison, the relative antibacterial activity of Mt_2-AgNPs was calculated as follows:

$$\text{Relative antibacterial activity} = \\ = 11.2/22.1 \times 100 \approx 50.7\%$$

Thus, under the experimental conditions used in this study, the antibacterial activity of the Mt_2-AgNPs sample was approximately 50.7% of that of erythromycin. It should be noted that erythromycin was used not as a direct functional analogue of the studied material, but as a standard positive control to validate the test system.

In addition, our result is comparable with literature data [19] reported an inhibition zone of 10.74 mm for an AgNPs–MMT system, which is close to the value obtained in our study (11.2 mm). The difference is 0.46 mm, or approximately 4.3%, indicating that the antibacterial activity of our material is consistent with previously reported silver-containing montmorillonite systems.

3.2 FTIR analysis

Figure 2 shows the comparative FTIR spectra of the pristine Mt_1 and Mt_2 samples and the AgNP-modified samples, Mt_1-AgNPs and Mt_2-AgNPs. For all samples, the intense absorption band in the 1000-1002 cm^{-1} region is attributed to Si-O stretching vibrations characteristic of smectites, particularly montmorillonite. The peak near 920 cm^{-1} corresponds to the deformation vibrations of Al–Al–OH/Al–OH groups in the octahedral layer. The peaks in the region of 517 cm^{-1} are attributed to the lattice vibrations of Si–O–Al and Al–O–Si bonds. The peak at 1445 cm^{-1} is attributed to the presence of carbonate salts in the mineral clay composition. The band at 1632 cm^{-1} is associated with the H–O–H bending vibrations of adsorbed or interlayer water, while the broad absorption region at 3463–3632 cm^{-1} is explained by the O–H stretching vibrations of structural

hydroxyl groups and physically bound water. Such a set of peaks confirms the aluminosilicate nature of bentonite, more specifically its layered structure rich in montmorillonite, and this interpretation is consistent with studies in which clay minerals were investigated by FTIR spectroscopy [20]. The preservation of the main characteristic peaks after the incorporation of silver nanoparticles indicates that the silicate framework of bentonite remained intact. These results suggest that silver-containing species may interact with the montmorillonite structure, possibly through partial intercalation without causing destruction of the basic aluminosilicate framework [21]. Studies by Praus, P. and Turicová, M. have shown that the intercalation of AgNPs into the clay matrix occurs while preserving the structural framework [22]. From a biomedical perspective, such structural preservation and surface functionalization are of great importance, since silver-modified montmorillonite systems of this kind are considered promising components for antimicrobial materials, drug delivery platforms, and composite materials for external wound applications [23]. The preservation of the main Si–O, Al–OH, and O–H vibration bands after the incorporation of silver nanoparticles indicates that the basic layered aluminosilicate framework of bentonite remained intact. At the same time, slight changes in the intensityrelated to O–H stretching and H–O–H bending vibrations may reflect changes in the hydration state of the clay and possible interactions between silver-containing species, surface hydroxyl groups, and interlayer water molecules [24-25]. Therefore, the FTIR results suggest that AgNP incorporation is accompanied by interaction with active sites of the montmorillonite structure. These interactions may contribute to the stabilization and dispersion of silver nanoparticles in the clay matrix, which is important for maintaining antibacterial functionality [26-27].

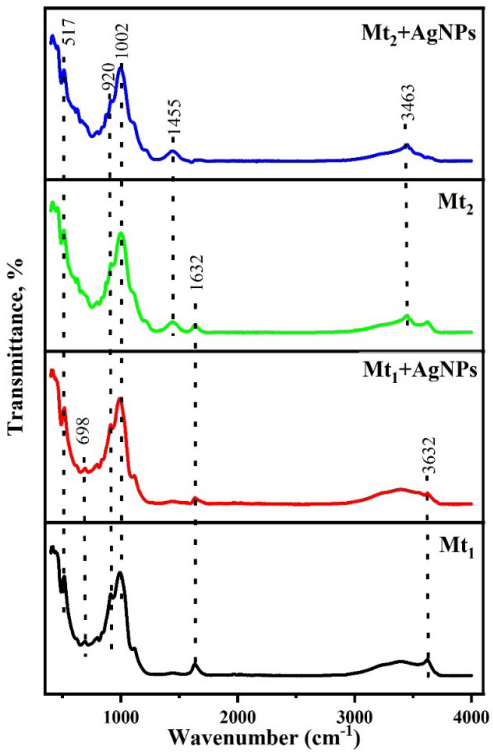

Figure 2. Comparative FTIR spectra of the initial Mt_1 and Mt_2 samples and the AgNP-modified samples, Mt_1-AgNPs and Mt_2-AgNPs.

3.3 XRF analysis

The comparative elemental composition of the pristine Mt_1 and Mt_2 samples, as well as the silver nanoparticle-modified Mt_1-AgNPs and Mt_2-AgNPs samples, is presented in the table. The obtained results indicate that the composition of the investigated samples is mainly represented by elements characteristic of aluminosilicate minerals. Si and Al were dominant in all samples, indicating that these elements constitute the main framework-forming com-

ponents. In particular, the pristine Mt_1 sample contained 25.021% Si, 8.315% Al, 2.119% Ca, 1.567% Fe, and 1.424% Mg, while the Mt_2 sample contained 26.989% Si, 9.017% Al, 4.991% Ca, 2.858% Fe, and 1.095% Mg. These values reflect the aluminosilicate nature of the studied samples and their elemental composition characteristic of clay minerals, including montmorillonitic materials. In addition, the presence of cation-exchangeable elements such as Ca, Mg, Fe, and K may positively contribute to the high sorption and ion-exchange properties of these materials [28].

After modification with silver nanoparticles, a slight decrease in the content of the major elements was observed in the Mt_1-AgNPs and Mt_2-AgNPs samples. For example, in the Mt_1-AgNPs sample, the Mg content decreased from 1.424% to 1.371%, Ca from 2.119% to 2.005%, Fe from 1.567% to 1.314%, and P from 0.444% to 0.412%. Similarly, in the Mt_2-AgNPs sample, the contents of Al, Si, Ca, and Fe were found to decrease from 9.017% to 8.099%, from 26.989% to 26.122%, from 4.991% to 4.361%, and from 2.858% to 2.658%, respectively. These changes can be explained by the partial substitution of weakly bound ions on the sample surface and in the interlayer space during the incorporation of silver nanoparticles, as well as by the restructuring of the surface layer [24].

In addition, the Ag content increased markedly after modification. Specifically, while the Ag content in the initial Mt_1 sample was only 0.003%, it increased to 0.312% in the Mt_1-AgNPs sample. A similar pattern was also observed in the Mt_2 system: the Ag content was 0.001% in the initial sample and increased to 0.297% in the Mt_2-AgNPs sample. These values confirm the successful immobilization of silver nanoparticles on the clay matrix surface and demonstrate the effectiveness of the modification process.

Table 2. Main elemental composition of the initial Mt_1 and Mt_2 samples and the AgNP-modified Mt_1-AgNPs and Mt_2-AgNPs samples.

Elements	Mt_1,%	Mt_1- AgNPs,%	Mt_2, %	Mt_2- AgNPs, %
Mg	1.424	1.371	1.095	1.071
Al	8.315	8.305	9.017	8.099
Si	25.021	25.001	26.989	26.122
P	0.444	0.412	0.412	0.365
K	0.078	0.052	0.132	0.06
Ca	2.119	2.005	4.991	4.361
Mn	0.119	0.105	0.157	0.147
Fe	1.567	1.314	2.858	2.658
Ag	0.003	0.312	0.001	0.297

3.4 X-ray diffraction analysis

Figure 3 shows the X-ray diffractograms of the initial Mt_1 and Mt_2 samples and the AgNP-modified samples, Mt_1-AgNPs and Mt_2-AgNPs. For the initial Mt_1 and Mt_2 samples, the intense reflection in the $2\theta = 26.5°$ (101) region is assigned to the quartz phase, while the peaks located at approximately 19.8° (110), 35.4° (200), and 62.3° (101) are characteristic of montmorillonite [20]. In the AgNP-modified Mt_1-AgNPs and Mt_2-AgNPs samples, the preservation of the main peaks of the aluminosilicate matrix indicates that the layered structure of bentonite remained intact during the modification process. Furthermore, the emergence of an additional peak in the $2\theta = 64–65°$ region is assigned to the (220) plane of the face-centered cubic (fcc) lattice of metallic silver. According to the studies of Shameli K. et al., in Ag/MMT-type systems the silver phase is typically characterized by peaks near 38.3° (111), 44.4° (200), 64.4° (220), and 77.7° (311) [24]; therefore, the observation of signals in these regions confirms the effective intercalation of AgNPs into the montmorillonite matrix.

The XRD results showed a shift of the basal reflection of montmorillonite toward lower 2θ values, accompanied by a slight increase in the interlayer distance d001 by approximately 0.0003–0.0006 nm. This change may indicate a partial expansion of the interlayer space and can be associated with the possible penetration of silver ions into the montmorillonite interlayer galleries.

Table 3. Changes in the interplane distance of the main peaks.

№	2 θ	d-spacing (Å)	2 θ	d-spacing (Å)	Δ d-spacing
	Main peaks of raw $Mt_{1,2}$		Main peaks of AgNP-$Mt_{1,2}$		
1	19.81	4.4715	19.79	4.48258	0.0110
2	35.03	2.55951	34.95	2.56519	0.0056
3	62.21	1.49107	62.05	1.49453	0.0034

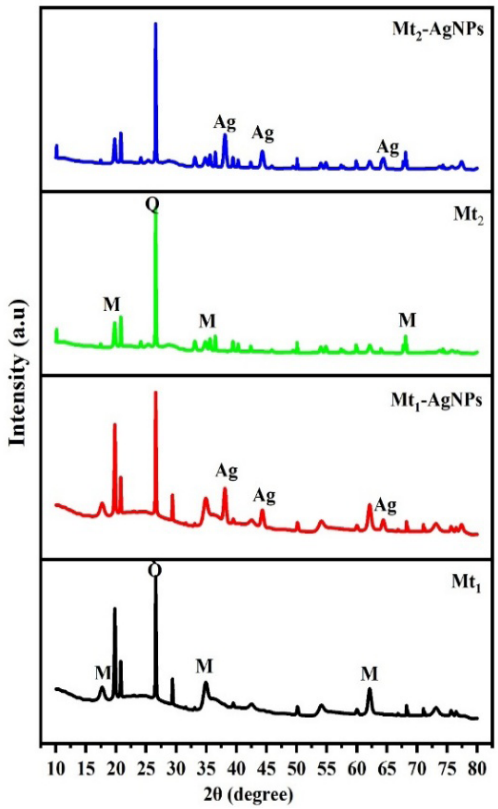

Figure 3. Comparative X-ray diffraction patterns of the initial Mt_1 a nd Mt_2 samples and the AgNP-modified Mt_1-AgNPs and Mt_2-AgNPs samples.

3.5 SEM images analysis

Figure 4 presents the SEM surface morphology of the initial Mt_1 and Mt_2 samples and the AgNP-modified Mt_1-AgNPs and Mt_2-AgNPs samples. The pristine Mt_1 and Mt_2 samples exhibited a morphology composed of agglomerated plate-like layers with a relatively irregular shape and a porous surface. In the present study, the particle size of the Mt_1 sample ranged from 805.4 nm to 1.540 μm, with an average of 1.22 μm, while that of the Mt_2 sample varied from 536.8 nm to 2.559 μm, with a mean value of 1.57 μm. These findings are in agreement with the submicron- and micron-sized ranges reported for montmorillonite particles in earlier studies [6,13,23], indicating that secondary agglomeration occurs in the pristine samples. After modification with silver nanoparticles, the overall layered morphology of the samples was preserved; however, the surface became denser, more compact, and more homogeneous. In particular, in the Mt_1-AgNPs sample, the shift in particle size to the range of 1.025–2.410 μm and the increase in the average value to 1.79 μm indicate that particle re-agglomeration and structural densification occurred after the introduction of AgNPs. Similar changes were also observed in the Mt_2-AgNPs sample, particularly surface smoothing and a closer packing of the layers. Such morphological transformations have likewise been reported for silver–montmorillonite composite systems [25].

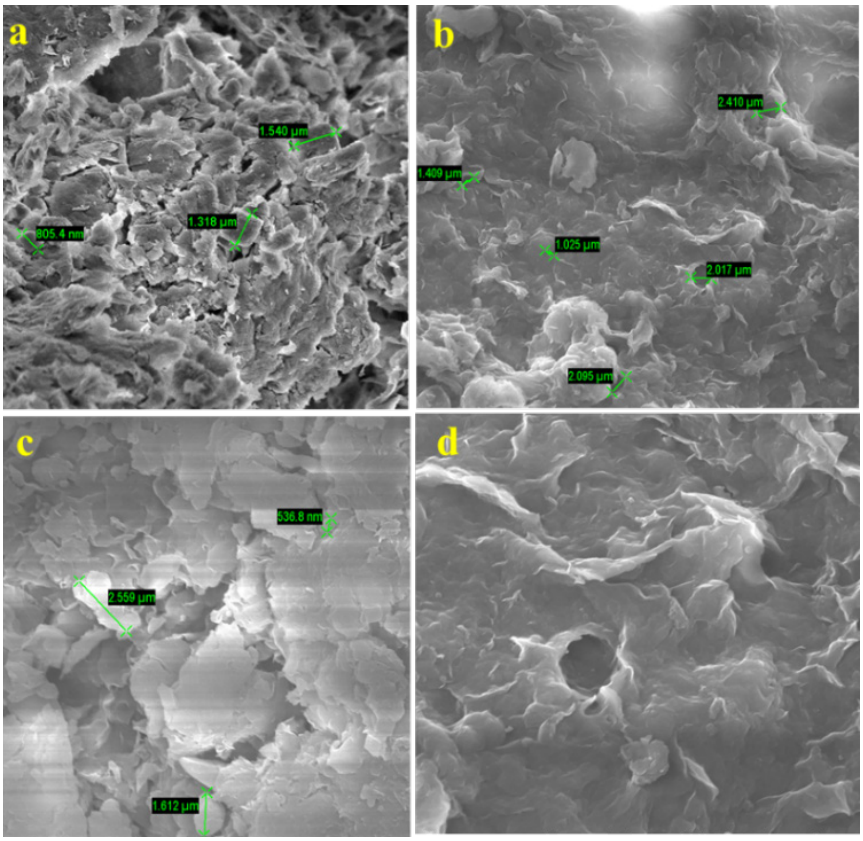

Figure 4. SEM images of the samples: (a) Mt_1, (b) Mt_1-AgNPs, (c) Mt_2, and (d) Mt_2-AgNPs.

3.6 Viscosity of the nanocomposite

The viscosity of the pristine Mt_1 and Mt_2 samples, as well as that of the AgNP-intercalated Mt_1-AgNPs and Mt_2-AgNPs samples, determined at room temperature, was 41.816, 39.994, 39.794, and 39.210 mPa·s, respectively. Following the incorporation of AgNPs, the viscosity decreased slightly, by 4.4% for Mt_1 and 1.5% for Mt_2. These findings suggest that the investigated systems retain a flowable dispersed state, which is favorable for facile application and uniform spreading on external wounds. For topical semisolid dosage forms, the rheological properties substantially affect the spreadability of the formulation, ease of application, release of the active component, and its penetration through the skin or wound surface. In this regard, the relatively low viscosity observed in the compositions studied in [28] may be regarded not as a drawback, but rather as a positive factor that contributes to improved spreadability of the composition, more effective contact of silver nanoparticles with the wound surface, and increased availability of the active phase. Therefore, montmorillonite material intercalated with silver nanoparticles may be regarded not as a classical high-viscosity ointment base, but rather as a promising matrix-forming agent for soft ointment or gel-ointment systems intended for external wound applications [29].

Table 4. Viscosity of the nanocomposite.

№	Mt_1	Mt_1-AgNPs	Mt_2	Mt_2-AgNPs
1	42.266 mPa·s	40.111 mPa·s	40.361 mPa·s	39.671 mPa·s
2	41.177 mPa·s	39.861 mPa·s	39.912 mPa·s	38.719 mPa·s
3	42.007 mPa·s	40.011 mPa·s	39.111 mPa·s	39.241 mPa·s
Average	41.816 mPa·s	39.994 mPa·s	39.794 mPa·s	39.210 mPa·s

Similar approaches to the evaluation of rheological properties of bentonite and clay-based systems have been reported in previous studies [30,31], where such materials were considered for topical drug delivery and semi-solid medical compositions.

Therefore, the viscosity analysis is relevant to the proposed application of the developed composite material.

4. Conclusion

The conducted studies made it possible to comprehensively evaluate the structural, morphological, and antibacterial properties of the Mt_1 and Mt_2 bentonite clays, as well as those of the silver nanoparticle-intercalated Mt_1-AgNPs and Mt_2-AgNPs samples. The FTIR, XRD, and SEM results showed that the main layered aluminosilicate framework of bentonite was preserved after modification, while the silver nanoparticles were distributed over the sample surface and within the interlayer space. According to the XRD data, the shift of the montmorillonite basal reflection and the slight increase in the interlayer distance may indicate the possible penetration of silver ions and/or silver-containing nanostructures into the interlayer space. The Mt_2-AgNPs sample obtained using 75 mL of AgNPs solution showed the highest antibacterial activity, with an inhibition zone of approximately 11–11.2 mm, under the experimental conditions used in this study, the antibacterial activity of the Mt_2-AgNPs sample was approximately 50.7% of that of erythromycin.This indicates its pronounced antibacterial effect. In addition, the microbiological purity of the investigated clay samples was found to comply with the requirements of the State Pharmacopoeia of the Republic of Kazakhstan. The viscosity of the modified samples, which remained within the range of 39–40 mPa·s, demonstrated their strong potential for rheological application as matrix materials in the development of soft dosage forms, including ointment compositions. The intercalation of silver nanoparticles promoted densification of the surface structure, morphological reorganization, and an increase in the functional activity of the samples. In general, the obtained findings suggest that silver nanoparticle-modified bentonite clays may be considered promising matrix materials for drug delivery systems, antimicrobial coatings, materials for external wound treatment, and the development of medicinal ointments.

Funding

This research has been funded by the Science Committee of the Ministry of Science and Higher Education of the Republic of Kazakhstan (Grant No. BR 24993105)

Conflicts of interest

The authors declare no conflict of interest.

Author contributions

Conceptualization: B.D.K. and K.A.; Methodology: K.A.; Software: B.D.K. and D.V.; Validation: K.A. and K.S.K.; Formal Analysis: B.D.K.; Investigation: M.Sh.A.; Resources. K.S.K. and A.K.; Data Curation: K.S.K. and A.K.; Writing – Original Draft Preparation: B.D.K. and K.A.; Writing – Review & Editing: K.S.K.; Visualization: B.D.K.; Supervision: K.A.; Project Administration: K.S.K.; Funding Acquisition.A.K. All authors have read and agreed to the published version of the manuscript.

References

1. D. Bolatkan, A. Kerimkulova, M. Beisebekov et al., "Quantitative assessment of the use of Kazakhstan montmorillonite clays as sorbent carriers for pharmaceutical substances," *Phys. Sci. Technol.*, vol. 12, no. 1–2, pp. 121–133, 2025. https://doi.org/10.26577/phst202512112

2. S. Saif, S. Mubeen, W. Abbass et al., "Exploring the feasibility of utilizing high plastic clays as an alternative material to bentonite clay in the production of ceramic tile: Advancing towards efficient life cycle cost," *Case Stud. Constr. Mater.*, vol. 20, 2024, Art. no. e03277. https://doi.org/10.1016/j.cscm.2024.e03277

3. W. A. Muslim, S. K. Al-Nasri, T. M. Albayati, and I. K. Salih, "Investigation of bentonite clay minerals as a natural adsorbents for Cs-137 real radioactive wastewater treatment," Desalin. Water Treat., vol. 317, 2024, Art. no. 100121. https://doi.org/10.1016/j.dwt.2024.100121

4. M. Skakov, "Highly efficient copper–palladium nanoalloy catalysts on modified carbon supports", *Phys. Sci. Technol.*, vol. 12, no. 3-4, pp. 10–27, Dec. 2025. https://doi.org/10.26577/phst202512

5. M. Bayandinova, A. . Kenesbekov, . A. Serikbaykyzy, . A. . Askhatov, Y. Batanov, and N. Bazarov, "Development of biocompatible coatings for orthopedic joint implants", *Phys. Sci. Technol.*, vol. 12, no. 1-2, pp. 84–94, Jun. 2025. https://doi.org/10.26577/phst20251218

6. M. Beisebekov, S. Kabdrakhmanova, N. Kantay et al., "Comparative study of a new sodium-bentonite clay for use in the pharmaceutical industry," *ES Mater. Manuf.*, vol. 30, 2025, Art. no. 1954. http://dx.doi.org/10.30919/mm1954

7. E. Srasra and I. Bekri-Abbes, "Bentonite clays for therapeutic purposes and biomaterial design," *Curr. Pharm. Des.*, vol. 26, 2020. https://doi.org/10.2174/1381612826666200203144034

8. M. S. Rana and S. Kim, "Bentonite in Korea: A resource and research focus for biomedical and cosmetic industries," *Materials*, vol. 17, no. 9, 2024, Art. no. 1982. https://doi.org/10.3390/ma17091982.

9. W. M. Alamier, M. Imran, S. K. Ali et al., "Synthesis of high-performance Fe_3O_4/graphene/bentonite clay nanocomposite for sustainable ciprofloxacin adsorption," *Inorg. Chem. Commun.*, vol. 174, pt. 1, 2025, Art. no. 113991. https://doi.org/10.1016/j.inoche.2025.113991

10. D. Luo and J. Wei, "Upgrading sodium montmorillonite into a reactive internal curing agent for sustainable cement composites through non-ionic functionalization," *Compos. Part B Eng.*, vol. 242, 2022, Art. no. 110076. https://doi.org/10.1016/j.compositesb.2022.110076

11. H. Tabasi, F. Oroojalian, and M. Darroudi, "Green clay ceramics as potential nanovehicles for drug delivery applications," *Ceram. Int.*, vol. 47, pp. 31042–31053, 2021. https://doi.org/10.1016/j.ceramint.2021.08.090

12. S. K. Kabdrakhmanova, A. Z. Kerimkulova, S. Z. Nauryzova et al., "Bentonite-based composites in medicine: Synthesis, characterization, and applications," *J. Compos. Sci.*, vol. 9, 2025, Art. no. 310. https://doi.org/10.3390/jcs9060310

13. T. Jamil, S. Yasin, N. Ramzan et al., "Bentonite-clay/CNT-based nano adsorbent for textile wastewater treatment: Optimization of process parameters," *Water*, vol. 15, no. 18, 2023, Art. no. 3197. https://doi.org/10.3390/w15183197

14. Y. Xing, X. Liao, X. Liu et al., "Characterization and antimicrobial activity of silver nanoparticles synthesized with the peel extract of mango," *Materials (Basel)*, vol. 14, no. 19, 2021, Art. no. 5878. https://doi.org/10.3390/ma14195878

15. A. Géloën, G. Mussabek, A. Kharin, T. Serdiuk, S. A. Alekseev, and V. Lysenko, "Impact of carbon fluoroxide nanoparticles on cell proliferation," *Nanomaterials*, vol. 11, no. 12, Art. no. 3168, Dec. 2021. https://doi.org/10.3390/nano11123168.

16. M. Isaiev, G. Mussabek, P. Lishchuk, K. Dubyk, N. Zhylkybayeva, G. Yar-Mukhmedova, D. Lacroix, and V. Lysenko, "Application of photoacoustic approach for characterization of nanostructured materials," *Nanomaterials*, vol. 12, no. 4, Art. no. 708, Feb. 2022. https://doi.org/10.3390/nano12040708.

17. N. Zhylkybayeva, K. Paliienko, A. Topchylo, A. Zaderko, A. Géloën, T. Borisova, L. Grishchenko, R. Mariychuk, V. Skryshevsky, G. Mussabek, and V. Lysenko, "Size dependent properties of Gd3+-free versus Gd3+-doped carbon dots for bioimaging application," *Sci. Rep.,* vol. 14, Art. no. 27812, Nov. 2024. https://doi.org/10.1038/s41598-024-76500-z.

18. J. Madejová, "FTIR techniques in clay mineral studies," *Vib. Spectrosc.*, vol. 31, no. 1, pp. 1–10, 2003. https://doi.org/10.1016/S0924-2031(02)00065-6

19. A. Mokhtar, A. B. Ahmed, B. Asli, B. Boukoussa, M. Hachemaoui, M. Sassi, and M. Abboud, "Recent advances in antibacterial metallic species supported on montmorillonite clay mineral: A review," *Minerals*, vol. 13, no. 10, 2023, Art. no. 1268. https://doi.org/10.3390/min13101268.

20. S. Z. Nauryzova, S. K. Kabdrakhmanova, A. K. Kabdrakhmanova et al., "Comprehensive study of silver nanoparticle functionalization of Kalzhat bentonite for medical application," *J. Compos. Sci.*, vol. 9, no. 12, 2025, Art. no. 702. https://doi.org/10.3390/jcs9120702

21. P. Praus, M. Turicová, V. Machovič, S. Študentová, and M. Klementová, "Characterization of silver nanoparticles deposited on montmorillonite," *Appl. Clay Sci.*, vol. 49, no. 3, pp. 341–345, 2010. https://doi.org/10.1016/j.clay.2010.06.009

22. S. Barakan, V. Aghazadeh, and M. Aghazadeh, "Separation and characterisation of montmorillonite from a low-grade natural bentonite using a non-destructive method," *Micro Nano Lett.*, 2019. https://doi.org/10.1049/mnl.2018.5364

23. M. Horue, M. L. Cacicedo, M. A. Fernandez et al., "Antimicrobial activities of bacterial cellulose–silver montmorillonite nanocomposites for wound healing," *Mater. Sci. Eng*. C, vol. 116, 2020, Art. no. 111152 https://doi.org/10.1016/j.msec.2020.111152

24. B. Tyagi, C. D. Chudasama, and R. V. Jasra, "Determination of structural modification in acid activated montmorillonite clay by FT-IR spectroscopy," *Spectrochim. Acta Part A Mol. Biomol. Spectrosc.*, vol. 64, no. 2, pp. 273–278, 2006. https://doi.org/10.1016/j.saa.2005.07.018.

25. K. Shameli et al., "Synthesis of silver nanoparticles in montmorillonite and their antibacterial behavior," *Int. J. Nanomedicine*, vol. 6, pp. 581–590, 2011. https://doi.org/10.2147/IJN.S17112.

26. K. Shameli, M. B. Ahmad, W. M. Z. W. Yunus et al., "Synthesis of silver/montmorillonite nanocomposites using γ-irradiation," *Int. J. Nanomedicine*, vol. 5, pp. 1067–1077, 2010. doi:10.2147/IJN.S15033

27. A. Agwu, A. Okorie, O. Akpanika, and A. Okon, "Activation of local bentonitic clays for use as viscosifiers in water-based drilling fluids," *J. Sci. Res. Rep*., vol. 12, pp. 1–11, 2016. https://doi.org/10.9734/JSRR/2016/28719.

28. A. Z. M. Badruddoza, M. I. Zahid, T. Walsh et al., "Topical drug delivery by Sepineo P600 emulgel: Relationship between rheology, physical stability, and formulation performance," *Int. J. Pharm.*, vol. 658, 2024, Art. no. 124210. https://doi.org/10.1016/j.ijpharm.2024.124210

29. Z. Rutkuniene, M. Balandyte, and G. Karbauskyte, "Formation of diamond like carbon films on materials for medical application", *Phys. Sci. Technol.*, vol. 8, no. 1-2, pp. 35–40, Jul. 2021. https://doi.org/10.26577/phst.2021.v8.i1.04

30. M. Ruggeri, R. Sánchez-Espejo, L. Casula, G. Sandri, L. Perioli, M. C. Cardia, et al., "Bentonite- and palygorskite-based gels for topical drug delivery applications," *Pharmaceutics*, vol. 15, 2023. https://doi.org/10.3390/pharmaceutics15041253.

31. M. N. Calienni, L. M. Martínez, M. C. Izquierdo, S. d. V. Alonso, and J. Montanari, "Rheological and viscoelastic analysis of hybrid formulations for topical application," *Pharmaceutics*, vol. 15, no. 10, p. 2392, 2023. https://doi.org/10.3390/pharmaceutics15102392.

Information about the authors:

Dana Bolatkan (corresponding author) – PhD student at S. Amanzholov East Kazakhstan University (Oskemen, Kazakhstan, email: chilibayeva35@gmail.com).

Kydyrmolla Akatan – PhD in chemistry, Head of the National Laboratory for Collective Use S. Amanzholov East Kazakhstan University (Oskemen, Kazakhstan, email: kidirmolla@gmail.com).

Kabdrakhmanova Sana Kanatbekovna – Candidate of Technical Sciences, Associate Professor, Director of the International R&D Center for Advanced Functional Materials and Their Composites, Satpaev University (Almaty, Kazakhstan, email: skabdrakhmanova@gmail.com).

Davydova Veronika – master student at Satpaev University, Junior researcher at International R&D Center for Advanced Functional Materials and Their Composites (Almaty, Kazakhstan, e-mail: veronikaspost17@gmail.com).

Muzdybayeva Sharbanu Akkazinovna – Candidate of Chemical Sciences and an Associate Professor at the Department of "Biochemical Engineering" of the International Engineering and Technology University (Almaty, Kazakhstan, e-mail: Sharbanu1958@mail.ru).